

# Organic Materials

## Research Progress of $\beta$ -Ketoenamine-Linked Covalent Organic Frameworks for Photocatalytic Hydrogen Evolution

Ping Xue, Mingyuan Li, Mi Tang, Zhengbang Wang, Chengliang Wang.

Affiliations below.

DOI: 10.1055/a-2291-8578

Please cite this article as: Xue P, Li M, Tang M et al. Research Progress of  $\beta$ -Ketoenamine-Linked Covalent Organic Frameworks for Photocatalytic Hydrogen Evolution. *Organic Materials* 2024. doi: 10.1055/a-2291-8578

**Conflict of Interest:** The authors declare that they have no conflict of interest.

**This study was supported by** National Natural Science Foundation of China (<http://dx.doi.org/10.13039/501100001809>), 52173163

### Abstract:

$\beta$ -ketoamide COFs, also named Tp-COFs, are considered to be a milestone material in the history of photocatalysts because of its excellent visible-light absorption, high crystallinity, ultra-high stability and structural diversity. In recent years, a large number of Tp-COFs and their composites were successfully constructed based on molecular or composite engineering strategies, and exhibited splendid photocatalytic water splitting activity. In comparison with composite strategy, molecular engineering technique effectively avoids interface problems by designing and preparing frameworks in the molecular level. Therefore, it is necessary to timely summarize the construction of Tp-COF photocatalysts based on molecular engineering strategy, so as to provide some theoretical basis and enlightenment for the subsequent development of high-performance Tp-COFs. Finally, the shortcomings and challenges of this technique and personal views on the further development of Tp-COFs are presented.

### Corresponding Author:

Prof. Chengliang Wang, Huazhong University of Science and Technology, School of Integrated Circuits, Luoyu Road 1037, 430074 Wuhan, China, [clwang@hust.edu.cn](mailto:clwang@hust.edu.cn)

### Affiliations:

Ping Xue, Hubei University of Science and Technology, Xianning Medical College, Xianning, China

Mingyuan Li, Wuhan University, College of Chemistry and Molecular Sciences, Wuhan, China

Mi Tang, Hubei University, School of Materials Science and Engineering, Wuhan, China

Zhengbang Wang, Hubei University, School of Materials Science and Engineering, Wuhan, China

Chengliang Wang, Huazhong University of Science and Technology, School of Integrated Circuits, Wuhan, China

# Research Progress of $\beta$ -Ketoenamine-Linked Covalent Organic Frameworks for Photocatalytic Hydrogen Evolution

Ping Xue<sup>1, #</sup>; Mingyuan Li<sup>4, #</sup>; Mi Tang<sup>3, \*</sup>; Zhengbang Wang<sup>3</sup>; Chengliang Wang<sup>2, \*</sup>

1. School of Pharmacy, Xianning Medical College, Hubei University of Science and Technology, Xianning, 437100, China

2. School of Integrated Circuits, Wuhan National Laboratory for Optoelectronics (WNLO), Huazhong University of Science and Technology, Wuhan 430074, China

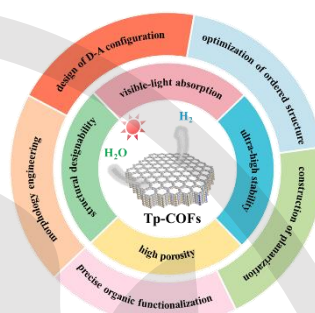
3. Ministry of Education Key Laboratory for the Green Preparation and Application of Functional Materials, Hubei Key Laboratory of Polymer Materials, Collaborative Innovation Center for Advanced Organic Chemical Materials Co-constructed by the Province and Ministry, School of Materials Science and Engineering, Hubei University, Wuhan, 430062, China

4. College of Chemistry and Molecular Sciences, Hubei Key Laboratory of Electrochemical Power Sources, Wuhan University, Wuhan, 430000, China

\*Corresponding email: clwang@hust.edu.cn; mtang@hbu.edu.cn

#These authors contributed equally to this work.

Ping Xue: writing – original draft. Mingyuan Li: writing – original draft. Mi Tang: review & editing. Zhengbang Wang: review & editing. Chengliang Wang: review & editing, project administration.



The modification of microstructure of  $\beta$ -ketoamide COFs, also known as Tp-COFs, exhibits great potential to construct high-performance photocatalysts.

Received:  
Accepted:  
Published online:  
DOI:

**Abstract**  $\beta$ -ketoamide COFs, also named Tp-COFs, are considered to be a milestone material in the history of photocatalysts because of its excellent visible-light absorption, high crystallinity, ultra-high stability and structural diversity. In recent years, a large number of Tp-COFs and their composites were successfully constructed based on molecular or composite engineering strategies, and exhibited splendid photocatalytic water splitting activity. In comparison with composite strategy, molecular engineering technique effectively avoids interface problems by designing and preparing frameworks in the molecular level. Therefore, it is necessary to timely summarize the construction of Tp-COF photocatalysts based on molecular engineering strategy, so as to provide some theoretical basis and enlightenment for the subsequent development of high-performance Tp-COFs. Finally, the shortcomings and challenges of this technique and personal views on the further development of Tp-COFs are presented.

**Key words**  $\beta$ -Ketoenamine; covalent organic frameworks; photocatalytic; hydrogen.

## Introduction

As a green and sustainable energy, hydrogen is one of the most promising alternative candidates for traditional fossil energy, and expected to solve the current energy crisis and severe environmental deterioration<sup>1</sup>. Among many approaches to hydrogen, the photocatalysis technology driven by inexhaustible solar energy undoubtedly offers a green and sustainable path<sup>2</sup>. It is worth to mentioning that there are three key processes in the photoinduced water splitting<sup>3</sup>: (a) the light adsorption of photocatalyst, (b) the separation and transfer of photoinduced charge-carriers in the catalyst, and (c) the acquisition of electrons by H<sup>+</sup> on the surface of the catalyst to form hydrogen. Therefore, the development of catalyst with high performance is one of the key scientific issues in this field. Over the past few decades, numerous types of photocatalysts have been reported, and the regulation and modification based on the structure, morphology structure and composite catalysts have been fully explored<sup>4</sup>.

Although some achievements have been made in the development of photocatalysts, there are still some defects<sup>5</sup>, such as the narrow light absorption, the recombination of photogenerated electron-charge pairs, low specific surface area and poor stability. Therefore, it is urgent to develop photocatalyst with strong visible-light absorption and high charge-carriers utilization, so as to realize efficient capture and utilization of solar energy and industrial application of photocatalytic water splitting. Covalent organic frameworks (COFs) are particularly prominent in the new generation of semiconductor photocatalysts due to their excellent visible-light absorption, structural designability, high permanent porosity and ultra-high physical and chemical stability<sup>5b, 6</sup>. Since Lotsch *et al.*<sup>7</sup> first reported a hydrazone-based COF as photocatalyst to achieve photocatalytic hydrogen evolution in 2014, a large numbers of COF-based photocatalysts have been successfully constructed for photocatalytic water splitting with amazing catalytic performances<sup>8</sup>. Among these COFs,  $\beta$ -ketoamide COFs (Tp-COFs, **Figure 1**) obtained by Schiff base reaction and irreversible enol-to-keto tautomerism with 1,3,5-triformylphloroglucinol (Tp) and amines as building block<sup>9</sup> exhibited preeminent hydrogen evolution activity<sup>4b, 8e, 10</sup>. The splendid photocatalytic activity of Tp-COFs may be related to the following factors: 1) the abundant conjugated structure broadens the light absorption range of the photocatalyst<sup>11</sup>; 2) the irreversible  $\beta$ -ketoamide bonds endow Tp-COFs with ultra-high thermal and chemical stability, which was conducive to maintaining the stability of the structure during catalysis<sup>9</sup>; 3) the carbonyl oxygen and enamine nitrogen atoms in the skeleton supplies binding sites for metal ions<sup>10f, 12</sup>; 4) the strong  $\pi$ - $\pi$  stacking between adjacent layers provides another path for charge-carriers transfer<sup>13</sup>; 5) the high porosity and specific surface area offers more active sites for catalytic reaction<sup>14</sup>; 6) the high crystallization reduces the recombination of photogenerated electron-hole pairs in bulk defects<sup>4a</sup> and offers more insight into the catalyst structure. At present, the optimization strategy of Tp-COFs catalysts mainly focuses on two

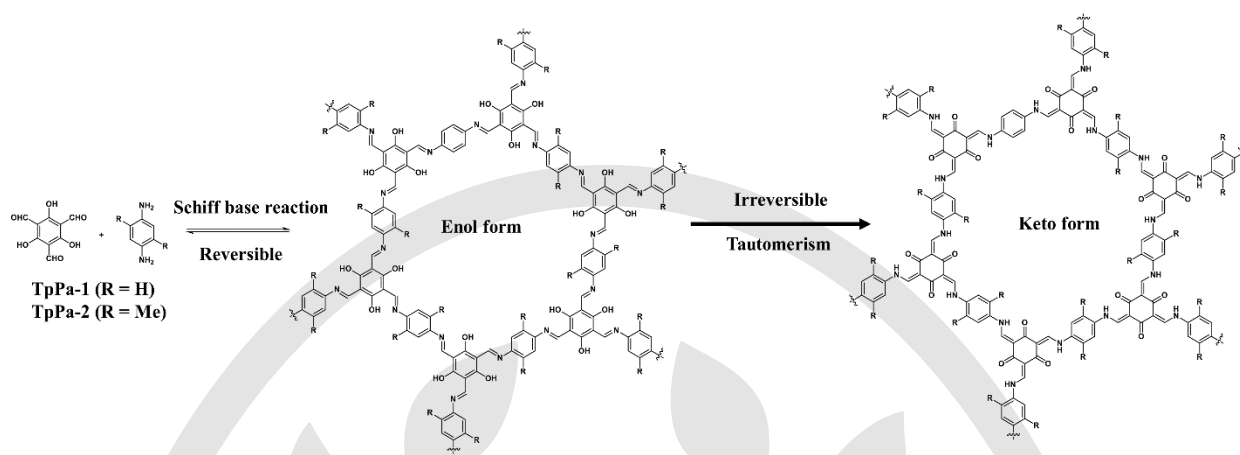


Figure 1. Schematic diagram of the synthesis of Tp-COFs (Tp-Pa-1 and 2).

points: molecular and composite engineering. In spite of the fact that the composite strategy is simple, general and easy to operate, some intrinsic properties such as the difficulty of forming a controllable composite interface and poor interface stability, still restricts the widespread application in the efficient photoinduced water splitting. By contrast, molecular engineering strategy shows more advantages in terms of regulable band structure and catalytic site at the molecular level. Thus, it is necessary to summarize the researches of Tp-COFs in photocatalytic hydrogen evolution based on molecular engineering strategy. Previous reviews of Tp-COFs focused on synthesis<sup>15</sup> and photocatalytic hydrogen evolution with a preference for composite engineering strategies<sup>16</sup>. Different from these reviews, this paper is dedicated to concentrating on Tp-COF photocatalysts from the perspective of molecular engineering, including the construction of planarization, optimization of ordered structure, precise organic functionalization and effect of morphology. Finally, we also provide an outlook of the challenges and some enlightenments for the subsequent construction of high-efficiency Tp-COF photocatalysts.

#### Brief introduction of synthesis of Tp-COFs

To achieve a wide-range application of Tp-COF photocatalysts, it is particularly important to develop convenient, economical and efficient synthesis methods. Additionally, since synthesis methods have a strong impact on the photocatalytic hydrogen evolution performance of Tp-COFs due to the different crystallinity, morphology and specific surface area, herein, the syntheses of Tp-COFs are also discussed and summarized in **Table 1**.

Generally, Tp-COFs are synthesized by solvothermal method. Specifically, all reactants are fully mixed in solvents and then seal in Pyrex tubes for 3 days or more at a certain temperature. In 2012, Banerjee *et al.*<sup>9</sup> first reported the successful synthesis of Tp-Pa-1/2 in mesitylene and dioxane solvents with acetic acid as catalyst in sealed Pyrex tubes at 120°C for 3 days. In the subsequent study, other common solvents, such as *N,N*-dimethylformamide (DMF), dimethyl sulfoxide (DMSO) and *N,N*-dimethylacetamide (DMAc), were also used to synthesize Tp-COFs<sup>13a, 17</sup>. Moreover, in 2017, Dichtel *et al.*<sup>18</sup> pre-protected diamines based on formal transamination strategy to obtain Tp-COF with ultra-high specific surface area (> 2600 m<sup>2</sup>/g). In 2019 and 2021, the crystallinity of Tp-COFs was improved by the construction of dynamic imine bonds<sup>19</sup>. Furthermore, In 2015,

Wang *et al.*<sup>20</sup> took microwave-assisted solvothermal method to quickly construct Tp-COFs within 60 min; however, sealing conditions and high boiling solvent were still required.

Although it was inclined to form good crystalline Tp-COFs via solvothermal method, the harsh reaction conditions and milligram-scale synthesis seriously limit its practical application. Banerjee research group has done a lot of outstanding works in the practical synthesis of Tp-COFs. In 2013, Banerjee *et al.*<sup>21</sup> efficiently prepared a series of Tp-COFs (TpPa-1, TpPa-1 and TpBD) with a graphene-like layered morphology through solvent-free mechanochemical synthesis (naming grinding method). Similarly, Tp-COFs nanosheets were also prepared by this method<sup>22</sup>, such as TpPa-F<sub>4</sub>, TpPa-(Me)<sub>2</sub>, TpPa-(OMe)<sub>2</sub>, TpPa-NO<sub>2</sub> and TpPa-(NO<sub>2</sub>)<sub>2</sub>. However, these COFs exhibited poor crystallinity and porosity. To improve crystallinity, this group also reported a liquid-assisted mechanochemical technique in the presence of trace amounts of solvent (so-called microsolution), such as DMF, *o*-dichlorobenzene and acetic acid,<sup>23</sup>. The microsolution was beneficial for dispersing reactants and thereby improving the crystallinity of Tp-COF to some extent. They also found that acid catalyst, such as *p*-toluenesulfonic, and Tp-COF precursors would help maintain the reversibility of COF formation reaction to prepare highly crystalline Tp-COFs<sup>24</sup>. Very recently, emulsion polymerization has also been used to construct Tp-COFs. This method can not only gently and fast produce COFs, but also avoid the use of acidic catalysts and a large number of organic solvents<sup>25</sup>.

Based on the actual demand of photocatalyst, such as easy recovery after the reaction and integration, the development of film-type COF catalysts is the trend. In recent years, due to the challenges of constructing stable, continuous, high crystalline and porous COF films, there have been relatively few reports on the preparation of Tp-COF films. In 2015, Wang *et al.*<sup>26</sup> demonstrated a one-way diffusion strategy to grow Tp-COF films on PEI-modified polyethersulfone (PES) substrates. In 2017, Banerjee *et al.*<sup>27</sup> successfully fabricated four Tp-COF films with high crystallinity and specific surface area at the dichloromethane/water interface via bottom-up interfacial strategy, also known as interface synthesis techniques. Recently, Agarwal *et al.*<sup>28</sup> reported the preparation of flexible self-standing Tp-COF membranes with high specific surface area and strong mechanical stability by the combination of electrospinning technology with solvothermal method.

Table 1. The synthesis method of Tp-COFs

Method	Condition	Product form	Advantage	Optimization method	Ref
solvothermal method	mesitylene, dioxane, acetic acid, 120°C, 3 d	powder	high crystallinity	replacement solvent, pre-protection, construction of dynamic imine bonds, microwave assisted	9, 13a, 17-20
mechanochemical method	1-2 drops of mesitylene: dioxane (1: 1), rt, 45 min	powder	rapid synthesis	liquid-assisted mechanochemical method	21-24
emulsion polymerization	CPB, dichloromethane, rt, 10 min	powder	rapid synthesis, high crystallinity and controlled morphology	-	25
interfacial strategy	dichloromethane, water, rt, 72 h, undisturbed condition	film	Film-type catalyst	-	27
electrospinning technology with solvothermal method	1. Pa/PAN film (electrospinning technology) 2. Tp-COF/PAN film (solvothermal method)	film	Film-type catalyst, self-standing film, high flexibility	-	28

CPB: cetylpyridinium bromide; Pa: *p*-phenylenediamine; PAN: polyacrylonitrile; rt: room temperature.

Therefore, in the subsequent design of high-performance Tp-COFs based on molecular engineering strategy, the selection of synthesis path is also particularly important. In addition, it is worth pointing out that the research of COF membranes is still in initial stage, and the development of Tp-COF-based plate reactor should be valued highly.

#### Optimization of photocatalytic hydrogen evolution by molecular engineering strategies

Due to the replaceability of the building blocks, COFs have more

opportunities for regulation and modification of photocatalytic activity at the molecular level. Based on regulations of group electronic properties, steric effect, conjugation degree and so on, it is easy to design Tp-COFs catalysts with different properties. Moreover, the molecular engineering strategy avoids the regulation of complicated interfaces. At present, Tp-COFs photocatalyst constructed by molecular engineering strategy exhibited excellent hydrogen evolution, which was summarized in **Table 2**. The structure optimization molecular engineering strategy mainly focus on the following aspects.

Table 2. The summary of the photocatalytic hydrogen evolution performance of Tp-COFs constructed by molecular engineering strategy.

COFs	Sacrificial agent	H <sub>2</sub> evolution rate (mmol·h <sup>-1</sup> ·g <sup>-1</sup> )	Light	Ref.
TP-EDDA	TEOA	0.324	λ > 395 nm	29
TP-BDDA	TEOA	0.03	λ > 395 nm	29
Tp-DTP	SA	4.76 μmol m <sup>-2</sup> h <sup>-1</sup>	λ > 400 nm	30
TpBD	SA	7.19 μmol m <sup>-2</sup> h <sup>-1</sup>	λ > 400nm	30
TpPa-H	SA	11.13 μmol m <sup>-2</sup> h <sup>-1</sup>	λ > 400 nm	30
TpPa-Cl <sub>2</sub>	SA	11.73 μmol m <sup>-2</sup> h <sup>-1</sup>	λ > 400 nm	30
TpPa-SO <sub>3</sub> H	SA	4.44 μmol m <sup>-2</sup> h <sup>-1</sup>	λ > 400 nm	30
TpPa-(CH <sub>3</sub> ) <sub>2</sub>	SA	3.62 μmol m <sup>-2</sup> h <sup>-1</sup>	λ > 400 nm	30
AntCOF-150	TEOA	0.055	λ > 395 nm	31
BtCOF-150	TEOA	0.75	λ > 395 nm	31
TpCOF-150	TEOA	0.05	λ > 395 nm	31
TzCOF-150	TEOA	0	λ > 395 nm	31
COF-BBT	SA	48.7	λ > 420 nm	32
S-COF	AA	4.44	λ > 420 nm	33

FS-COF	AA	10.1	$\lambda > 420$ nm	33
BT-COF <sup>a</sup>	AA	2.02	$\lambda > 420$ nm	34
BT-COF <sup>b</sup>	AA	7.7	$\lambda > 420$ nm	34
30%PEG@BT-COF	AA	11.14	$\lambda > 420$ nm	34
RC-COF-1	AA	27.98	$\lambda > 420$ nm	35
COF-935	AA	67.55	$\lambda > 420$ nm	36
<i>e</i> -Tp-Pa-COF	AA	133.9	AM 1.5	25
TpBpy-Ni2%	AA	51.3	$\lambda > 420$ nm	37
Tp-DB-(OCH <sub>3</sub> ) <sub>2</sub>	SA	1.23	$\lambda > 400$ nm	10g
Tp-DB-(CH <sub>3</sub> ) <sub>2</sub>	SA	0.81	$\lambda > 400$ nm	10g
Tp-DB	SA	0.60	$\lambda > 400$ nm	10g
Tp-DB-(NO <sub>2</sub> ) <sub>2</sub>	SA	0.015	$\lambda > 400$ nm	10g
TpPa-COF	SA	1.56	$\lambda > 420$ nm	38
TpPa-COF-NO <sub>2</sub>	SA	0.22	$\lambda > 420$ nm	38
TpPa-COF-(CH <sub>3</sub> ) <sub>2</sub>	SA	8.33	$\lambda > 420$ nm	38
Tp-DBN	SA	1.8	$\lambda > 420$ nm	10h
Pt@TpBpy-NS <sup>c</sup>	-	0.132	$\lambda > 420$ nm	39
Pt@TpBpy-2-NS <sup>c</sup>	-	41.3	$\lambda > 420$ nm	39
Tp-2C/BPy <sup>2+</sup> -COF	AA	34.6	$\lambda > 420$ nm	8a
BT-COF	AA	3.40	$\lambda > 420$ nm	40
HBT-COF	AA	19.00	$\lambda > 420$ nm	40
COF-H	AA	5.03	AM 1.5	41
COF-Cl	AA	5.84	AM 1.5	41
COF-F	AA	10.58	AM 1.5	41
CYANO-COF	AA	60.85	$\lambda > 420$ nm	42
CYANO-CN	AA	134.2	$\lambda > 420$ nm	42
BD-COF	AA	19.75	$\lambda > 420$ nm	42
BD-CN	AA	79.5	$\lambda > 420$ nm	42
TpBT-COF	AA	1.447	$\lambda > 420$ nm	43
Tp(BT <sub>0.5</sub> TP <sub>0.5</sub> )-COF	AA	9.839	$\lambda > 420$ nm	43
Tp(BT <sub>0.25</sub> TP <sub>0.75</sub> )-COF	AA	7.398	$\lambda > 420$ nm	43
Tp(BT <sub>0.1</sub> TP <sub>0.9</sub> )-COF	AA	5.822	$\lambda > 420$ nm	43
Tp(BT <sub>0.05</sub> TP <sub>0.95</sub> )-COF	AA	5.695	$\lambda > 420$ nm	43
TpTP-COF	AA	6.04	$\lambda > 420$ nm	43
2Me-OMe-COF	AA	33.1	$\lambda > 420$ nm	44
Me-2OMe-COF	AA	19.5	$\lambda > 420$ nm	44
TP-TTA/SiO <sub>2</sub> -1	AA	153.2	$\lambda > 420$ nm	45

<sup>a</sup> acetic acid as catalyst; <sup>b</sup> pyrrolidine as catalyst; <sup>c</sup> overall water splitting; TEOA: triethanolamine; SA: sodium ascorbate; AA: ascorbic acid. Pt co-catalyst was used unless otherwise illustrated.

### (1) The construction of planarization

It was been proved that the improvement of structural conjugation would reduce the coulomb binding force of electrons and holes, thereby increasing the exciton dissociation rate<sup>46</sup>.

Therefore, the introduction of highly conjugated units is one of the effective ways to improve the performance of COF photocatalysts. In 2017, Thomas' group successfully synthesized the acetylene-bridged COFs (Tp-EDDA and Tp-BDDA,



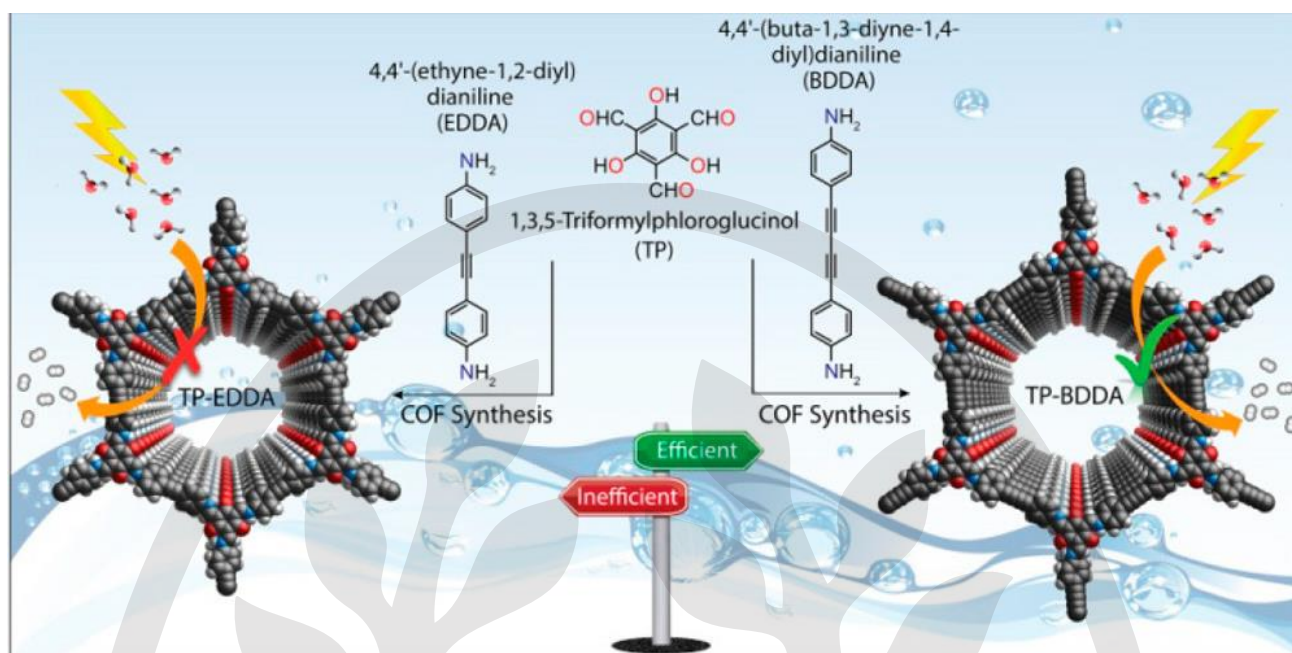


Figure 2. Structures of Tp-EDDA and TP-BDDA. Reprinted with permission from Ref. 29. Copyright 2018 American Chemical Society.

Figure 2) of which highly conjugated structure endowed charge-carriers with super mobility<sup>29</sup>. It was worth noting that the hydrogen evolution of Tp-BDDA (diacetylene-containing COF) was much better than that of Tp-EDDA (acetylene-containing COF). This indicates the diacetylene fraction has a profound effect on the photocatalytic activity of COFs, and the conjugated diacetylene moiety could accelerate the electron transformation, that is, the photogenerated excitons are more likely to migrate to the surface of the photocatalyst.

Subsequently, in 2021, Li *et al.* reported<sup>30</sup> that the photocatalytic performance of  $\beta$ -keto-enamine-based COFs decayed along with the length of the diamine linker (TpPa-H: 11.13  $\mu\text{mol m}^{-2} \text{h}^{-1}$ ; TpBD: 7.19  $\mu\text{mol m}^{-2} \text{h}^{-1}$ ; Tp-DTP: 4.76  $\mu\text{mol m}^{-2} \text{h}^{-1}$ ), mainly due to the fact that the increase of Tp-COF's torsion angles reduced the conjugation and planarity of the backbone, thus expanding the band gap and hindering carrier transfer and separation.

Besides, Seki and partners prepared four Tp-COFs with different torsion angles between central aromatic ring and peripheral benzene ring (Ant, 66°; Bt, 39°; Tp, 27°; Tz, 0°, Figure 3) by condensation of Tp with 4,4'-diamino-substituted *p*-terphenyl or its analogous derivatives<sup>31</sup>. It was found that the crystallinity (AntCOF150, amorphous; BtCOF150, semicrystalline; TpCOF150, semicrystalline and TzCOF150, crystalline) as well as specific surface area of these Tp-COFs were improved with the decrease of torsion angle in the building blocks. Unexpectedly, only BtCOF150 showed the highest hydrogen evolution in the presence of 1 wt% Pt as a cocatalyst in all constructed Tp-COFs. Apart from torsional angle, donor-acceptor (D-A) structure is also key factors for photocatalytic hydrogen production. The lowest unoccupied molecular orbital (LUMO) suffers from fall with the increase of the acceptor strength, resulting in insufficient driving force of TzCOF for hydrogen evolution. Recently, Li *et al.*

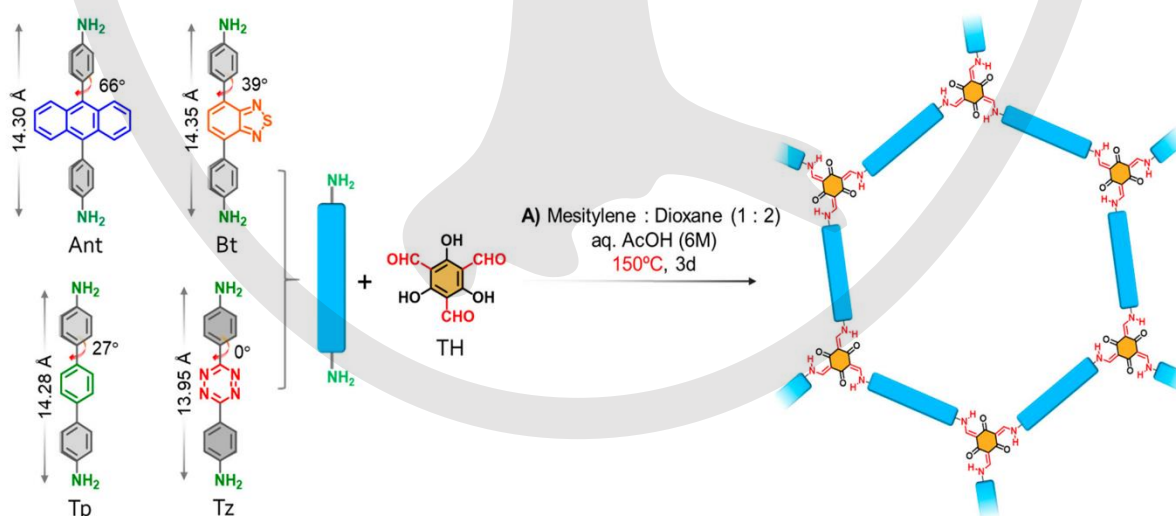


Figure 3. The synthesis and structures of Tp-COFs (AntCOF150, BtCOF150, TpCOF150 and TzCOF150; (150 represent the reaction temperature). Adapted with permission from Ref. 31. Copyright 2020 American Chemical Society.

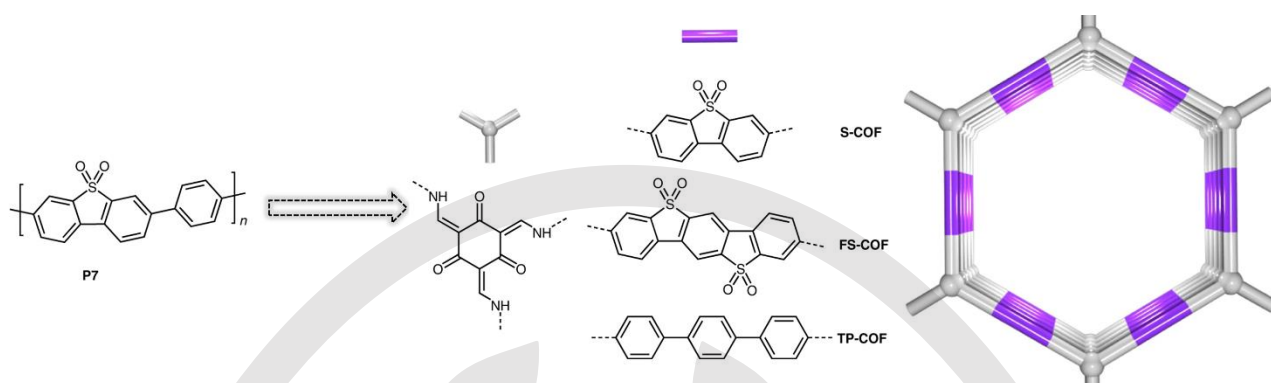


Figure 4. Structures and construction ideas of P7, S-COF and FS-COF. Adapted with permission from Ref. 8e. Copyright 2018 Springer nature.

reported<sup>32</sup> a Tp-COF contained benzobisthiazole (BBT) units with high crystallinity and wettability showed excellent photocatalytic performance ascribing to the enhanced interlayer electron delocalization and  $\pi$ - $\pi$  stacking by rigid and planar BBT unit.

## (2) Optimization of ordered structure

Generally, the crystallinity of materials is one of the most important factors in photogenerated carriers migration<sup>47</sup>. For instance, amorphous organic conjugated polymers exhibit local charge transport properties, partially due to local structural deformation caused by the disordered nature of the polymer blends<sup>48</sup>. Because of the long-range ordered structure, COFs

usually show the delocalized electronic states, which facilitate electron transport and intensify the reaction kinetics by the aggregation of photogenerated electrons. Therefore, in recently years, the research on organic photocatalysts has gradually shifted from amorphous and semi-crystalline polymers to crystalline COFs. For example, in 2016, Cooper group fused phenylenes by the introduction of bridging functionality (dibenzo[*b,d*]thiophene sulfone, DBTS) to prepare linear conjugated copolymer (**P7**, **Figure 4**)<sup>46b</sup> with high photocatalytic hydrogen evolution activity ( $1.49 \text{ mmol g}^{-1} \text{ h}^{-1}$ ) and an apparent quantum yield as high as 2.3% at 420 nm. The high photocatalytic

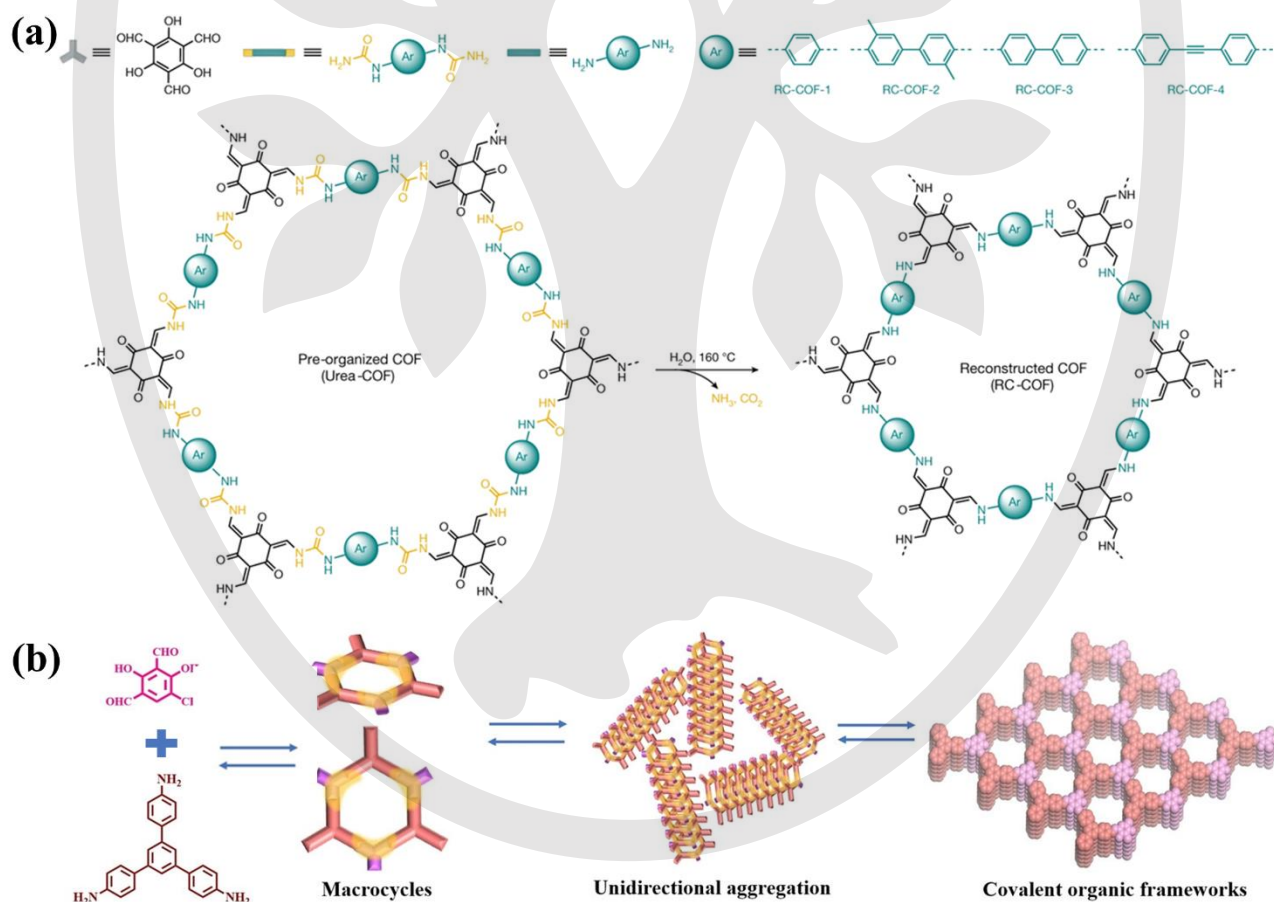


Figure 5. (a) Schematic diagram of the synthesis of RC-COFs by molecular reconstruction strategy. Adapted with permission from Ref. 35. Copyright 2023 Springer nature. (b) Growth mechanism diagram of COF-935 by dynamic imine bonds. Adapted with permission from Ref. 36. Copyright 2023 Wiley.

activity was attributed to the fact that the rigid DBTS units in the P7 copolymer accelerated the generation and transport of charge carriers, as mentioned above. Then, in 2018, this group set out to incorporate the DBTS unit into ordered Tp-COF on the basis of semi-crystalline **P7**, and successfully synthesized a sulfone-containing COFs (S-COF and FS-COF, **Figure 4**)<sup>8e</sup>. They found that the crystallinity of FS-COF was much better than that of S-COF due to fused and extended planar linker in FS-COF. As a result, the hydrogen evolution of high crystallinity FS-COF ( $10.1 \text{ mmol g}^{-1} \text{ h}^{-1}$ ) strongly outperformed that of relatively low crystalline S-COF ( $4.44 \text{ mmol g}^{-1} \text{ h}^{-1}$ ) and semi-crystalline copolymer **P7** ( $1.49 \text{ mmol g}^{-1} \text{ h}^{-1}$ ). As a contrast, the amorphous FS-COF analogue (FS-P) was also synthesized. As expected, the amorphous FS-P displayed much lower photocatalytic activity, with HER of only  $1.49 \text{ mmol g}^{-1} \text{ h}^{-1}$ . Furthermore, the photocatalytic activity of FS-COF was still preserved when it was cast on the substrate in the form of thin film.

Besides, two strategies including monomer exchange (based on dynamic imine bonds) and molecular reconstruction were also used to improve the crystallinity of Tp-COFs, and great successes have been achieved. In 2021, Guo *et al.*<sup>19a</sup> adopted pyrrolidine instead of acetic acid as catalyst to enhance the controllability of crystal growth kinetic by monomer exchange strategies<sup>19b</sup> and, in consequence, Tp-COFs with better crystallinity were acquired. The follow-up research exhibited that the photocatalytic activity of low crystalline BT-COF (acetic acid as catalyst,  $2.02 \text{ mmol g}^{-1} \text{ h}^{-1}$ ) was far less than that of high crystalline BT-COF (pyrrolidine as catalyst,  $7.7 \text{ mmol g}^{-1} \text{ h}^{-1}$ )<sup>34</sup>. Cooper *et al.*<sup>35</sup> found that framework reconstruction featuring synchronous hydrolysis of COFs and *in-situ* polymerization was beneficial to improve the crystallinity of COF. Based on this, ultra-high crystallinity RC-COF-1 was synthesized by the reaction of Tp and urea (**Figure 5a**), which showed the photocatalytic hydrogen evolution as high as  $27 \text{ mmol g}^{-1} \text{ h}^{-1}$ . The authors speculated high crystallinity brought up fast carrier transfer.

Moreover, the irreversible enol-to-keto tautomerization and dynamic imine bonds played an important role in improving COF ordered structures. For instance, high crystalline COF-935 was rapidly synthesized based on the formation of hexagonal intermediates (**Figure 5b**)<sup>36</sup>. The dynamic imine bond helped to maintain the reversibility of COF formation, which provided an opportunity for the modification and reconstruction of the framework. As a result, when it was exposed to visible light, COF-935 exhibited extremely high hydrogen evolution up to  $67.55 \text{ mmol g}^{-1} \text{ h}^{-1}$  with 3 wt% Pt as cocatalyst. More interesting, the

hydrogen evolution of COF-935 was still as high as  $19.80 \text{ mmol g}^{-1} \text{ h}^{-1}$  with 0.1 wt% Pt.

Herein, it should be briefly stated that the crystallinity of COF in the process of photocatalytic reaction was very likely to be destroyed owing to the disruption of stack order by breaking partial  $\pi$ - $\pi$  stacking between adjacent layers. Therefore, it is often observed that both XRD diffraction peaks and photocatalytic activities of COFs decreased after photocatalysis<sup>7, 49</sup>. In other word, the dislocation between adjacent layers breaks the  $\pi$ -stacking array, resulting in imitation of charge carrier transport. In 2021, Guo group<sup>34</sup> proposed to use linear polymer PEG to fill one-dimensional pores of BT-COF to stabilize and enhance the  $\pi$ -stacking of COF, as a consequence that PEG@BT-COF deposited by Pt displayed excellent hydrogen performance of  $11.14 \text{ mmol g}^{-1} \text{ h}^{-1}$ , which was almost 1.5 times that of pristine BT-COF. This result was attributed to the fact that the filled polyethylene glycol (PEG) was anchored to the framework of BT-COF via H-bonds and thereby inhibited the sliding of COF adjacent layers during Pt-cocatalyst deposition (**Figure 6**). As a result, the PEG@BT-COF photocatalytic material facilitated charge carrier transfer and extended exciton lifetime. Recently, this group<sup>37</sup> weakened the interlayer interaction of Tp-Bpy-COF by solvothermal method to transform the twist bipyridine part into a planar conformation, thereby favoring of the coordination with Ni<sup>2+</sup>. The obtained TpBpy-Ni2%-COF displayed outstanding hydrogen evolution up to  $51.3 \text{ mmol g}^{-1} \text{ h}^{-1}$ , and still had hydrogen production capacity under 700 nm light irradiation. The panchromatic photocatalytic hydrogen evolution derives from the coaxially ordered stacking that facilitated the coordination between metal ions and COF frameworks, thus promoting the metal-to-ligand transfer (MLCT).

### (3) Precise organic functionalization strategy

It is clear that functional substituents on the COFs framework with the different electron push-pull properties will affect the band gap of COFs as well as light absorption and exciton dissociation for photogenic electron transfer. Two studies have reported that the introduction of electron-donating functional groups into Tp-COFs enhanced  $\pi$  electron delocalization of Tp-COF skeletons. The enhanced  $\pi$  electron delocalization optimized charge carriers transport between and/or within covalent layers<sup>10g, 38</sup>, resulting in better photocatalytic hydrogen evolution. Meanwhile, the strongly electronegative substituents can also reinforce  $\pi$  electron delocalization over COF framework and accelerate photo-induced exciton dissociation by strengthening the polarization of the local charges<sup>50</sup>. In 2021, Li and co-workers introduced electron-withdrawing groups (-Cl and -SO<sub>3</sub>H) into TpPa-H to obtain TpPa-Cl<sub>2</sub> and TpPa-SO<sub>3</sub>H<sup>30</sup>, where TpPa-Cl<sub>2</sub> had superior hydrogen evolution ( $11.73 \mu\text{mol m}^{-2} \text{ h}^{-2}$ ) and apparent quantum efficiency (17%, 400 nm). This result was attributed to the strong electron-withdrawing ability of halogens, reasonable band structure, high carrier separation and so on. Besides halogens, the cyano is also a typical electron-withdrawing group. In 2021, Chen *et al.*<sup>10h</sup> reported a cyano-conjugation Tp-DBN-COF (**Figure 7a**) via aldehyde-imine Schiff-base condensation between Tp and 2,5-diaminobenzonitrile (DBN). The functionalized Tp-DBN-COF showed better photocatalytic hydrogen evolution (Tp-DBN-COF:  $1.8 \text{ mmol g}^{-1} \text{ h}^{-1}$ ; Tp-PDA-COF:  $0.6 \text{ mmol g}^{-1} \text{ h}^{-1}$ ) in comparison with the pristine Tp-PDA (Tp-Pa-1). The DFT calculation results revealed that the introduction of cyano to the backbones redistributed electrons in the  $\pi$ -conjugated framework and reduced the energy barrier generated

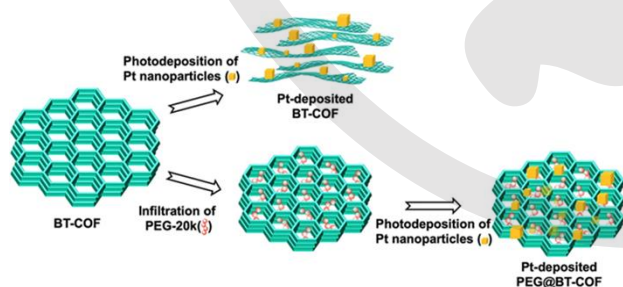


Figure 6. Schematic diagram of structural transformation of BT-COF and PEG@BT-COF during cocatalyst (Pt) deposition. Adapted with permission from Ref. 34. Copyright 2021 Springer nature.



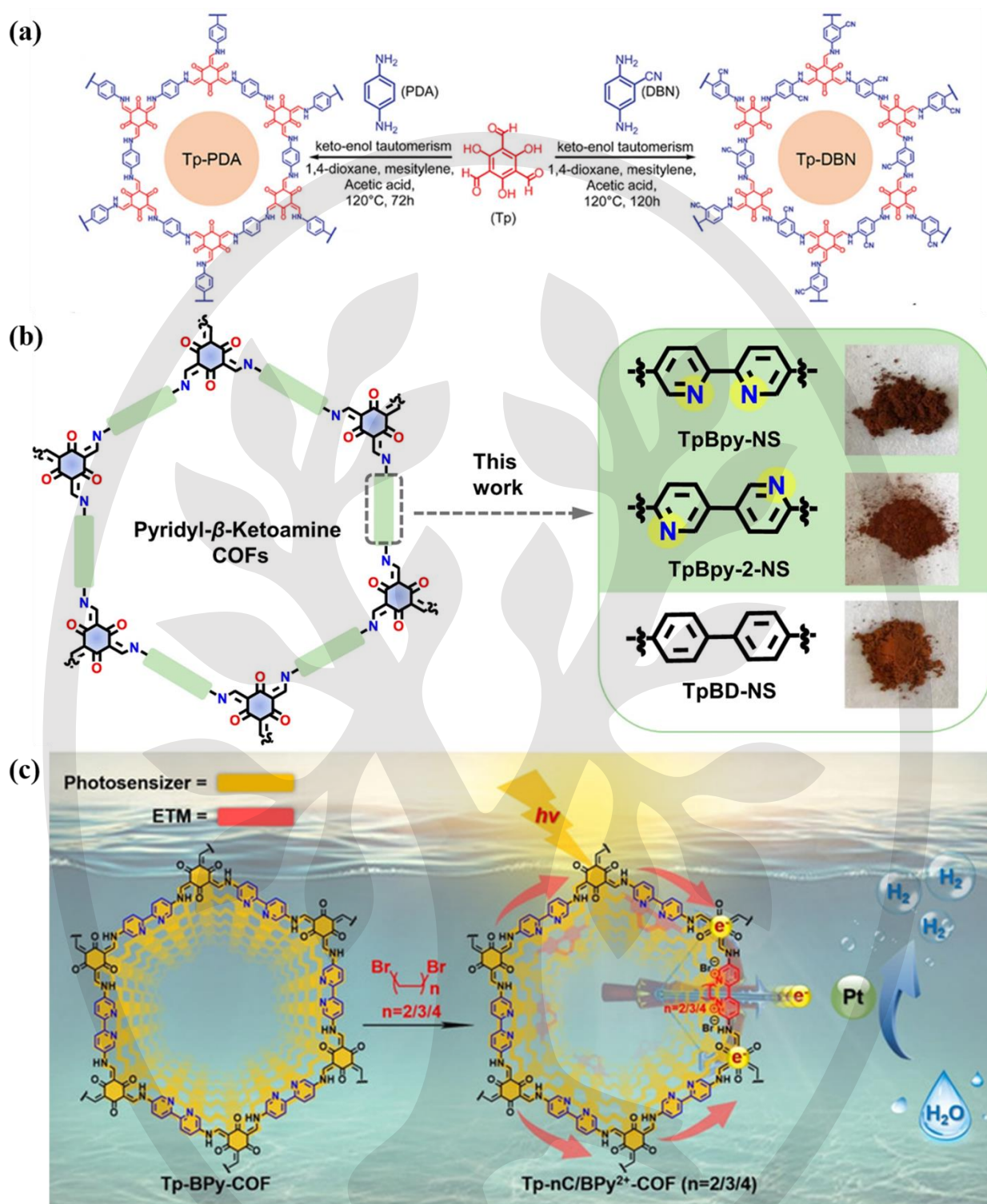


Figure 7. (a) Schematic illustration of the synthesis of Tp-COFs (Tp-PDA and Tp-DBN). Adapted with permission from Ref. 10h. Copyright 2018 Wiley. (b) Structures of Tp-COFs (Tp-Bpy-NS, Tp-Bpy-2-NS, Tp-BD-NS). Adapted with permission from Ref. 39. Copyright 2023 Springer nature. (c) Schematic diagram for Tp-nC/BPy<sup>2+</sup>-COF accelerating electron transfer. Reprinted with permission from Ref. 8a. Copyright 2021 Wiley.

by H-intermediate. It is worth noting that most of the current COFs don't show activity for photocatalytic overall water splitting because oxygen evolution reaction (OER) involves the sluggish four electrons process<sup>51</sup>. Some pioneering work has demonstrated that photocatalysts with N-containing aromatic heterocyclic structure could realize overall water splitting, such

as g-C<sub>3</sub>N<sub>4</sub><sup>52</sup> and covalent triazine frameworks (CTFs)<sup>53</sup>. Inspired by this, in 2023, Lan group introduced two bipyridine-containing fragments into Tp-COFs (Figure 7b), and found that Pt@TpBpy-NS and Pt@TpBpy-2-NS displayed activity of overall water splitting. However, Pt@TpBD-NS containing biphenyl fragments only exhibited drive hydrogen half-reactions activity<sup>39</sup>. Further

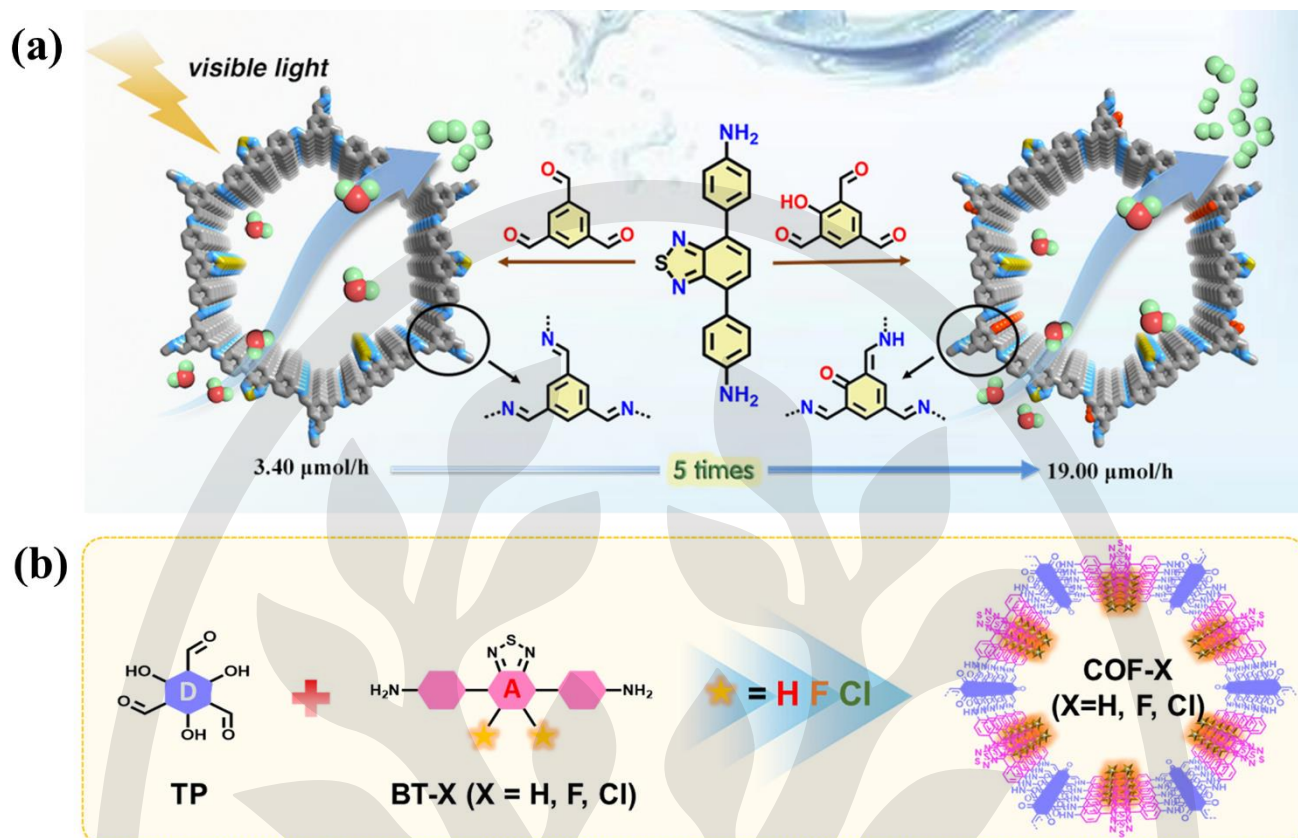


Figure 8. (a) Structures of BT-COF and HBT-COF. Reprinted with permission from Ref. 40. Copyright 2021 American Chemical Society. (b) TP-BT-X-COFs (X = H, F and Cl). Adapted with permission from Ref. 41. Copyright 2023 American Chemical Society.

study showed that the N-sites position in dipyrrolyl section had an important effect on the electron transfer from dipyrrolyl to Tp, which made the  $sp^2$ -hybridized C2 active sites more favorable to OER path. The functional COFs mentioned above all originate from pre-designed building blocks. However, it is difficult to synthesize structurally diverse functional building blocks. Hence, post-synthetic functionalization strategy offers a general approach to introduce a broad range of functional fragments into COFs without changing the ordered structure of COFs. By post-synthesis strategy, Guo *et al.*<sup>8a</sup> incorporated the electron transfer module (viologen derivatives) into Tp-COF and constructed a dual-function Tp-nC/BPy<sup>2+</sup>-COF with photosensitizing and electron transfer units. The synergistic effect of dual modules accelerates the carrier mobility and the overall reaction kinetics (Figure 7c), resulting in the excellent activity (34.6  $\text{mmol g}^{-1} \text{h}^{-1}$ ) of Tp-2C/BPy<sup>2+</sup>-COF under visible-light irradiation.

The design of D-A conformation based on electron regulation is also an important idea for precise organic functionalization strategy. In D-A structure, a strong dipole moment is generated and build-in electric field is formed to drive electrons from D to A due to the obvious different electron affinities between D and A, so as to improve the excitons dissociation and mobility of carriers<sup>54</sup>. So far, the design of D-A configuration has made great achievements on photocatalysis<sup>55</sup>, including Tp-COFs. In 2021, Zhuang group constructed D-A type HBT-COF and BT-COF by Schiff-base condensation of benzene-1,3,5-tricarbaldehyde (BT) and 2-hydroxybenzene-1,3,5-tricarbaldehyde (HBT) or 4,4'-(Benzo[c][1,2,5]thiadiazole-4,7-diyl)dianiline contained strong electron unit (benzothiadiazole moiety), respectively<sup>40</sup> (Figure 8a). Notably, HBT-COF presented superior hydrogen evolution

activity, which was ascribed to the introduction of hydroxyl groups to enhance the D-A effect and wettability. Meanwhile, the introduction of hydroxyl group derived a partial transformation of imine bonds into  $\beta$ -ketoamide structure, as a consequence that the crystallinity of HBT-COF was optimized to facilitate electron transfer. Li and co-workers constructed Tp-COFs (COF-Cl and COF-F, Figure 8b) with strong D-A effect by introducing electronegative Cl or/and F atoms into the benzothiadiazole moiety<sup>41</sup>. The incorporation of halogen atoms enhanced the intrinsic driving force for charge separation. In addition, due to the intramolecular hydrogen bond between F and hydrogen atom on the adjacent aromatic rings, the structure of COF-F was more planarity, further facilitating charge transport, as described above. In a similar way, Li *et al.*<sup>42</sup> replaced benzidine (BD) with 4,4'-diamino-[1,1'-biphenyl]-3,3'-dicyanitrile as the building block to obtain CYANO-COF with ketene-cyano (D-A) pair, and acquired COFs nanosheets (CYANO-CON) by ball milling. In the comparison with bulk CYANO-COF and H<sub>2</sub>BD-CON (nanosheets), CYANO-CON nanosheets showed higher photocatalytic activity with apparent quantum yield of CYANO-CON at 450 nm reaching up to 82.6%, which was one of the highest efficiencies so far. It could be ascribed to that the introduction of cyanide group shortens band group, enhances light capture, and constructs D-A pair to facilitate charge separation. In addition, the nanosheets also play a key role in shortening the distance of carrier transport and exposing more active sites.

The synergistic effect of multi-component building blocks in COF can further modulate the D-A structure to increase exciton dissociation. For example, Guo *et al.*<sup>43</sup> reported  $\beta$ -ketoenamine-linked Tp(BT<sub>x</sub>TP<sub>1-x</sub>)-COFs obtained by condensation 4,4'-

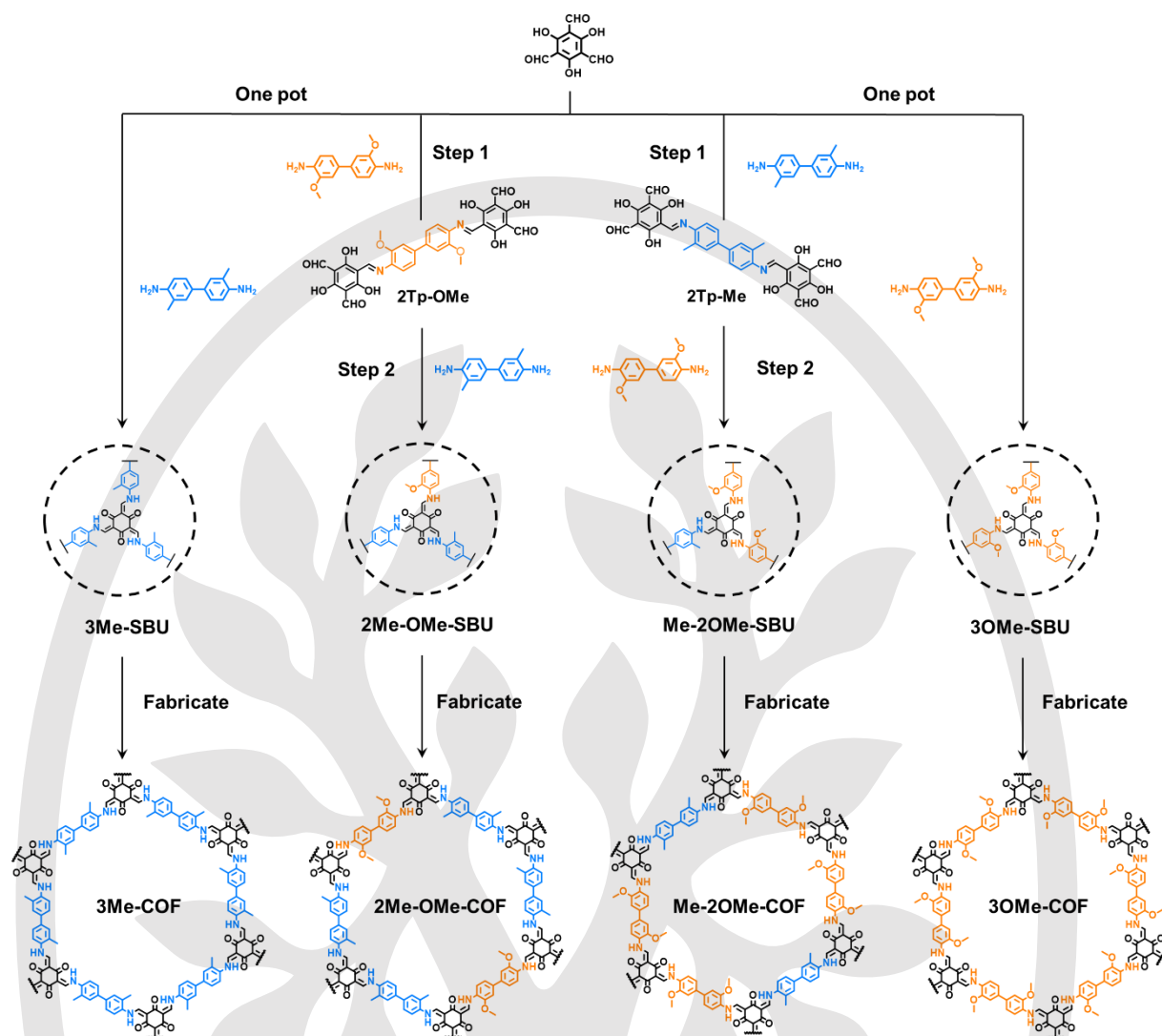


Figure 9. Schematic diagram of the synthesis of multi-component Tp-COFs. Adapted with permission from Ref. 44. Copyright 2023 Springer.

diamino-*p*-terphenyl (TP) and 4,4'-(benzo-2,1,3-thiadiazole-4,7-diyl)dianiline (BT) units with Tp as a fixed node. The D-A pair produced by the introduction of electronegative BT accelerated the exciton dissociation. However, with the further increase of BT content, the formation of the induced excimer state acted as exciton trap site and inhibited the long-distance diffusion of excitons to the catalytic sites. Although this multi-component COF owns good crystallinity, the local structure of COF is not clear from the microscopic point of view, which hinders the study of actual structure-activity relationship and runs counter to the original intention of COF structure precision. For this reason, the synthesis of multi-component ordered COFs is extremely urgent and full of challenges. In 2023, Jiang's group creatively adopted a hierarchical synthesis strategy to pre-polymerized the two building blocks according to stoichiometric ratios, and then assembled them with the third building block to form COFs (Figure 9)<sup>44</sup>. This approach reduced the complexity of ternary polymerization and achieved precise control at the binary level. As a result, both of 2Me-OMe-COF and Me-2OMe-COF exhibited remarkable hydrogen evolution activity, which could be attributed to multi-factor coupling such as absorbance, crystallinity and charge transport capacity; besides, the presence of D<sub>1</sub>-A-D<sub>2</sub> structure in COF might also affect the electron transfer

path.

#### (4) Effect of morphology

It has been mentioned above that the reduction of charge-carrier transmission distance could effectively improve its utilization. Therefore, the preparation of single-layer or few-layers is also an important candidate to reduce the recombination of photoinduced carriers. In 2022, Yang *et al.*<sup>45</sup> reported that Tp-COF colloid were deposited on strong affinity carrier (SiO<sub>2</sub>) in a self-exfoliating way to get a near-single layer COF (SLCOF, TP-TTA/SiO<sub>2</sub>-1). The near-SLCOF exhibited remarkable hydrogen evolution rate, up to 153.2 mmol g<sup>-1</sup> h<sup>-1</sup>, which was one of the highest hydrogen evolution performances so far. Deposition of near monolayer COF on the carrier not only reduced the number of expensive COFs, but also shortened the migration distance of photogenerated charge-carriers, thus improving the efficiency of photocatalysis.

Recently, Jin and co-workers successfully prepared high crystallinity TpPa-COF with different morphologies (spheres, bowls and fibers) by emulsion polymerization (Figure 10)<sup>25</sup>. The spherical morphology with higher specific surface area exposed more active sites and the smaller size COF shortened the carrier transport distance. As a result, the *e*-TpPa-COF (sphere



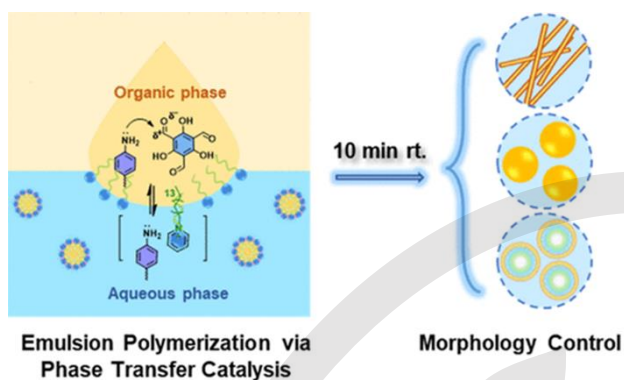


Figure 10. Schematic diagram of the synthesis of Tp-COFs by emulsion polymerization. Reprinted with permission from Ref. 25. Copyright 2020 American Chemical Society.

morphology) showed the best hydrogen evolution of  $133.9 \text{ mmol g}^{-1} \text{ h}^{-1}$  (with fresh emulsion and 0.9w% Pt), which was comparable to the most advanced COFs reported to date.

### Conclusions and outlook

The unique properties of Tp-COFs endow them with the potential to be prominent photocatalysts. Moreover, with the continuous exploration of the synthesis of Tp-COFs, large-scale and simple preparation has been realized, so the improvement of Tp-COFs' photocatalytic efficiency is a key factor to achieve its industrial applications. To date, Tp-COFs and its composites displayed excellent photocatalytic hydrogen evolution rate, surging new highs again and again. The construction and modification based on molecular engineering strategy are more likely to obtain high-performance Tp-COF photocatalysts because it maintains maximum crystallinity and avoids interface problems. Therefore, this paper reviews the research process of Tp-COFs based on molecular engineering strategy, so as to bring theoretical guidance for follow-up optimization.

Even if the construction of Tp-COF photocatalyst based on molecular engineering strategy possesses unparalleled advantages, the following challenges still seriously hinder its development. 1) Since the structure-activity relationship of Tp-COFs has not been fully defined, there is insufficient guidance for the design of high-activity Tp-COF photocatalysts. 2) Due to great challenge in the preparation of multi-component Tp-COFs with specific microstructure, the expected hydrogen evolution effect can't be achieved through multi-component regulation. 3) So far, most of the researches on photocatalytic hydrogen evolution were focused on the half-reaction for the reason that it is very difficult to achieve simultaneous hydrogen and oxygen evolution by synergistically regulating the band structure and catalytic sites. It runs counter to the original intention of developing photocatalyst. Therefore, the realization of Tp-COFs photocatalytic overall water splitting is also one of the key scientific problems to be solved urgently. 4) The construction of film-typed Tp-COF photocatalysts is on the primary stage, and the development of commercial plate reactor still seems a long way off. Therefore, more attention should be paid to the structure-activity relationship, the synthesis of multi-component Tp-COFs, Tp-COFs photocatalytic overall water splitting and the

development of plate reactor in follow-up research, so as to accelerate the industrial application of Tp-COF photocatalysts.

### Funding Information

This work was supported by the National Natural Science Foundation of China (52173163), the National 1000-Talents Program, the Innovation Fund of WNLO, Huazhong University of Science and Technology (HUST, 2023BR021), Hubei Provincial Natural Science Foundation of China (Project No. 2023AFB479) and the Hubei University of Science and Technology Doctoral Research Initiation Project (Project No. BK202325). The authors thank Project Funded by China Postdoctoral Science Foundation ((2022M710849 and 2023T160137), Department of Education of Hubei Province (Q20221004) and Overseas Expertise Introduction Center for Discipline Innovation (D18025).

### Conflict of Interest

There are no conflicts to declare.

### References

- (1) (a) Ni, M.; Leung, M. K. H.; Sumathy, K.; Leung, D. Y. C., *Int. J. Hydrogen Energy* **2006**, *31* (10), 1401-1412; (b) Abe, J. O.; Popoola, A. P. I.; Ajenifuja, E.; Popoola, O. M., *Int. J. Hydrogen Energy* **2019**, *44* (29), 15072-15086.
- (2) Lin, L.; Hisatomi, T.; Chen, S.; Takata, T.; Domen, K., *Trends Chem* **2020**, *2* (9), 813-824.
- (3) Abe, R., *J. Photoch. Photobio. C* **2010**, *11* (4), 179-209.
- (4) (a) Kong, M.; Li, Y.; Chen, X.; Tian, T.; Fang, P.; Zheng, F.; Zhao, X., *J. Am. Chem. Soc.* **2011**, *133* (41), 16414-16417; (b) Zhang, F. M.; Sheng, J. L.; Yang, Z. D.; Sun, X. J.; Tang, H. L.; Lu, M.; Dong, H.; Shen, F. C.; Liu, J.; Lan, Y. Q., *Angew. Chem. Int. Ed.* **2018**, *57* (37), 12106-12110; (c) Li, L.; Yan, J.; Wang, T.; Zhao, Z.-J.; Zhang, J.; Gong, J.; Guan, N., *Nat. Commun.* **2015**, *6* (1), 5881; (d) Zhou, Q.; Guo, Y.; Zhu, Y., *Nat. Catal.* **2023**, *6* (7), 574-584; (e) Zheng, X.; Feng, L.; Dou, Y.; Guo, H.; Liang, Y.; Li, G.; He, J.; Liu, P.; He, J., *ACS Nano* **2021**, *15* (8), 13209-13219; (f) Weng, W.; Guo, J., *Nat. Commun.* **2022**, *13* (1), 5768.
- (5) (a) Osterloh, F. E., *Chem. Soc. Rev.* **2013**, *42* (6), 2294-2320; (b) Freund, R.; Zaremba, O.; Arnauts, G.; Ameloot, R.; Skorupskii, G.; Dincă, M.; Bavykina, A.; Gascon, J.; Ejsmont, A.; Goscińska, J.; Kalmutzki, M.; Lächelt, U.; Ploetz, E.; Diercks, C. S.; Wuttke, S., *Angew. Chem. Int. Ed.* **2021**, *60* (45), 23975-24001; (c) Luo, T.; Gilmanova, L.; Kaskel, S., *Coord. Chem. Rev.* **2023**, *490*, 215210.
- (6) (a) Banerjee, T.; Bennett, T.; Butler, K.; Easun, T. L.; Eddaoudi, M.; Forgan, R.; Gagliardi, L.; Hendon, C.; Jorge, M.; Lamberti, C.; Lee, J.-S. M.; Leus, K.; Li, J.; Lin, W.; Ranocchiari, M.; Rosi, N.; Santacarla, J. G.; Shevlin, S.; Svane, K.; Ting, V.; van der Veen, M.; Van Der Voort, P.; Walsh, A.; Woods, D.; Yaghi, O. M.; Zhu, G., *Faraday Discuss.* **2017**, *201* (0), 87-99; (b) Zhang, F.; Li, X.; Dong, X.; Hao, H.; Lang, X., *Chinese J. Catal.* **2022**, *43* (9), 2395-2404; (c) Xiong, K.; Zhang, F.; Wang, Y.; Zeng, B.; Lang, X., *J. Colloid Interface Sci.* **2023**, *643*, 340-349.
- (7) Stegbauer, L.; Schwinghammer, K.; Lotsch, B. V., *Chem. Sci.* **2014**, *5* (7), 2789-2793.
- (8) (a) Mi, Z.; Zhou, T.; Weng, W.; Unruangsri, J.; Hu, K.; Yang, W.; Wang, C.; Zhang, K. A. I.; Guo, J., *Angew. Chem. Int. Ed.* **2021**, *60* (17), 9642-9649; (b) Zhong, Y.; Dong, W.; Ren, S.; Li, L., *Adv. Mater.* **2023**, e2308251; (c) Guan, X.; Qian, Y.; Zhang, X.; Jiang, H.-L., *Angew. Chem. Int. Ed.* **2023**, *62* (31), e202306135; (d) Wang, S.; Wu, T.; Wu, S.; Guo, J.; He, T.; Wu, Y.; Yuan, W.; Zhang, Z.; Hua, Y.; Zhao, Y., *Angew. Chem. Int. Ed.* **2023**, *62* (44), e202311082; (e) Wang, X.; Chen, L.; Chong, S. Y.; Little, M. A.; Wu, Y.; Zhu, W.-H.; Clowes, R.; Yan, Y.; Zwiijnenburg, M. A.; Sprick, R. S.; Cooper, A. I., *Nat. Chem.* **2018**, *10* (12), 1180-1189.
- (9) Kandambeth, S.; Mallick, A.; Lukose, B.; Mane, M. V.; Heine, T.; Banerjee, R., *J. Am. Chem. Soc.* **2012**, *134* (48), 19524-7.



- (10) (a) Ming, J.; Liu, A.; Zhao, J.; Zhang, P.; Huang, H.; Lin, H.; Xu, Z.; Zhang, X.; Wang, X.; Hofkens, J.; Roeffaers, M. B. J.; Long, J., *Angew. Chem. Int. Ed.* **2019**, *58* (50), 18290-18294; (b) Ding, S.-Y.; Wang, P.-L.; Yin, G.-L.; Zhang, X.; Lu, G., *Int. J. Hydrogen Energy* **2019**, *44* (23), 11872-11876; (c) Dong, H.; Meng, X.-B.; Zhang, X.; Tang, H.-L.; Liu, J.-W.; Wang, J.-H.; Wei, J.-Z.; Zhang, F.-M.; Bai, L.-L.; Sun, X.-J., *Chem. Eng. J.* **2020**, *379*, 122342; (d) Zhang, Y.-P.; Tang, H.-L.; Dong, H.; Gao, M.-Y.; Li, C.-C.; Sun, X.-J.; Wei, J.-Z.; Qu, Y.; Li, Z.-J.; Zhang, F.-M., *J. Mater. Chem. A* **2020**, *8* (8), 4334-4340; (e) Yao, Y.-H.; Li, J.; Zhang, H.; Tang, H.-L.; Fang, L.; Niu, G.-D.; Sun, X.-J.; Zhang, F.-M., *J. Mater. Chem. A* **2020**, *8* (18), 8949-8956; (f) Xue, P.; Pan, X.; Huang, J.; Gao, Y.; Guo, W.; Li, J.; Tang, M.; Wang, Z., *ACS Appl. Mater. Interfaces* **2021**, *13* (50), 59915-59924; (g) Xue, P.; Chen, W.; Tang, M.; Wang, Z.; Wang, Z., *Mol. Catal.* **2023**, *535*, 112807; (h) Wang, L.; Zhang, L.; Lin, B.; Zheng, Y.; Chen, J.; Zheng, Y.; Gao, B.; Long, J.; Chen, Y., *Small* **2021**, *17* (24), 2101017; (i) Li, Y.; Karimi, M.; Gong, Y.-N.; Dai, N.; Safarifard, V.; Jiang, H.-L., *Matter* **2021**, *4*, 2230-2265; (j) Li, C.-C.; Gao, M.-Y.; Sun, X.-J.; Tang, H.-L.; Dong, H.; Zhang, F.-M., *Appl. Catal. B Environ.* **2020**, *266*, 118586; (k) Zhang, F.; Xiong, K.; Lang, X., *ChemCatChem* **2023**, *15* (24), e202301179.
- (11) Wu, Z.; Huang, X.; Li, X.; Hai, G.; Li, B.; Wang, G., *Sci. China Chem.* **2021**, *64* (12), 2169-2179.
- (12) Wu, X.; Han, X.; Liu, Y.; Liu, Y.; Cui, Y., *J. Am. Chem. Soc.* **2018**, *140* (47), 16124-16133.
- (13) (a) Gao, M.-Y.; Li, C.-C.; Tang, H.-L.; Sun, X.-J.; Dong, H.; Zhang, F.-M., *J. Mater. Chem. A* **2019**, *7* (35), 20193-20200; (b) Karthik, P.; Vinoth, R.; Zhang, P.; Choi, W.; Balaraman, E.; Neppolian, B., *ACS Appl. Energy Mater.* **2018**, *1* (5), 1913-1923.
- (14) Zhang, H.-Y.; Yang, Y.; Li, C.-C.; Tang, H.-L.; Zhang, F.-M.; Zhang, G.-L.; Yan, H., *J. Mater. Chem. A* **2021**, *9* (31), 16743-16750.
- (15) Li, Y.; Liu, M.; Wu, J.; Li, J.; Yu, X.; Zhang, Q., *Front. Optoelectron.* **2022**, *15* (1), 38.
- (16) Wang, L.-J.; Dong, P.-Y.; Zhang, G.; Zhang, F.-M., *Energy Fuels* **2023**, *37* (9), 6323-6347.
- (17) Bhadra, M.; Kandambeth, S.; Sahoo, M. K.; Addicoat, M.; Balaraman, E.; Banerjee, R., *J. Am. Chem. Soc.* **2019**, *141* (15), 6152-6156.
- (18) Vitaku, E.; Dichtel, W. R., *J. Am. Chem. Soc.* **2017**, *139* (37), 12911-12914.
- (19) (a) Wang, R.; Kong, W.; Zhou, T.; Wang, C.; Guo, J., *Chem. Commun.* **2021**, *57* (3), 331-334; (b) Daugherty, M. C.; Vitaku, E.; Li, R. L.; Evans, A. M.; Chavez, A. D.; Dichtel, W. R., *Chem. Commun.* **2019**, *55* (18), 2680-2683.
- (20) Wei, H.; Chai, S.; Hu, N.; Yang, Z.; Wei, L.; Wang, L., *Chem. Commun.* **2015**, *51* (61), 12178-12181.
- (21) Biswal, B. P.; Chandra, S.; Kandambeth, S.; Lukose, B.; Heine, T.; Banerjee, R., *J. Am. Chem. Soc.* **2013**, *135* (14), 5328-5331.
- (22) Chandra, S.; Kandambeth, S.; Biswal, B. P.; Lukose, B.; Kunjir, S. M.; Chaudhary, M.; Babaroo, R.; Heine, T.; Banerjee, R., *J. Am. Chem. Soc.* **2013**, *135* (47), 17853-17861.
- (23) Shinde, D. B.; Aiyappa, H. B.; Bhadra, M.; Biswal, B. P.; Wadge, P.; Kandambeth, S.; Garai, B.; Kundu, T.; Kurungot, S.; Banerjee, R., *J. Mater. Chem. A* **2016**, *4* (7), 2682-2690.
- (24) (a) Karak, S.; Kumar, S.; Pachfule, P.; Banerjee, R., *J. Am. Chem. Soc.* **2018**, *140* (15), 5138-5145; (b) Karak, S.; Kandambeth, S.; Biswal, B. P.; Sasmal, H. S.; Kumar, S.; Pachfule, P.; Banerjee, R., *J. Am. Chem. Soc.* **2017**, *139* (5), 1856-1862.
- (25) Zhang, J.; Cheng, C.; Guan, L.; Jiang, H.-L.; Jin, S., *J. Am. Chem. Soc.* **2023**, *145* (40), 21974-21982.
- (26) Wang, R.; Wei, M.; Wang, Y., *J. Membr. Sci.* **2020**, *604*, 118090.
- (27) Dey, K.; Pal, M.; Rout, K. C.; Kunjattu H. S.; Das, A.; Mukherjee, R.; Kharul, U. K.; Banerjee, R., *J. Am. Chem. Soc.* **2017**, *139* (37), 13083-13091.
- (28) Ding, C.; Breunig, M.; Timm, J.; Marschall, R.; Senker, J.; Agarwal, S., *Adv. Funct. Mater.* **2021**, *31* (49), 2106507.
- (29) Pachfule, P.; Achariya, A.; Roeser, J.; Langenhahn, T.; Schwarze, M.; Schomäcker, R.; Thomas, A.; Schmidt, J., *J. Am. Chem. Soc.* **2018**, *140* (4), 1423-1427.
- (30) Yin, L.; Zhao, Y.; Xing, Y.; Tan, H.; Lang, Z.; Ho, W.; Wang, Y.; Li, Y., *Chem. Eng. J.* **2021**, *419*, 129984.
- (31) Ghosh, S.; Nakada, A.; Springer, M. A.; Kawaguchi, T.; Suzuki, K.; Kaji, H.; Baburin, I.; Kuc, A.; Heine, T.; Suzuki, H.; Abe, R.; Seki, S., *J. Am. Chem. Soc.* **2020**, *142* (21), 9752-9762.
- (32) Huang, W.; Hu, Y.; Qin, Z.; Ji, Y.; Zhao, X.; Wu, Y.; He, Q.; Li, Y.; Zhang, C.; Lu, J.; Li, Y., *Nat. Sci. Rev.* **2022**, *10* (1), nwa171.
- (33) Wang, X.; Chen, L.; Chong, S. Y.; Little, M. A.; Wu, Y.; Zhu, W.-H.; Clowes, R.; Yan, Y.; Zwijnenburg, M. A.; Sprick, R. S.; Cooper, A. I., *Nat. Chem.* **2018**, *10* (12), 1180-1189.
- (34) Zhou, T.; Wang, L.; Huang, X.; Unruangsri, J.; Zhang, H.; Wang, R.; Song, Q.; Yang, Q.; Li, W.; Wang, C.; Takahashi, K.; Xu, H.; Guo, J., *Nat. Commun.* **2021**, *12* (1), 3934.
- (35) Zhang, W.; Chen, L.; Dai, S.; Zhao, C.; Ma, C.; Wei, L.; Zhu, M.; Chong, S. Y.; Yang, H.; Liu, L.; Bai, Y.; Yu, M.; Xu, Y.; Zhu, X.-W.; Zhu, Q.; An, S.; Sprick, R. S.; Little, M. A.; Wu, X.; Jiang, S.; Wu, Y.; Zhang, Y.-B.; Tian, H.; Zhu, W.-H.; Cooper, A. I., *Nature* **2022**, *604* (7904), 72-79.
- (36) Wang, K.; Zhong, Y.; Dong, W.; Xiao, Y.; Ren, S.; Li, L., *Angew. Chem. Int. Ed.* **2023**, *62* (30), e202304611.
- (37) Zhang, H.; Lin, Z.; Kidkhunthod, P.; Guo, J., *Angew. Chem. Int. Ed.* **2023**, *62* (21), e202217527.
- (38) Sheng, J.-L.; Dong, H.; Meng, X.-B.; Tang, H.-L.; Yao, Y.-H.; Liu, D.-Q.; Bai, L.-L.; Zhang, F.-M.; Wei, J.-Z.; Sun, X.-J., *ChemCatChem* **2019**, *11* (9), 2313-2319.
- (39) Yang, Y.; Chu, X.; Zhang, H.-Y.; Zhang, R.; Liu, Y.-H.; Zhang, F.-M.; Lu, M.; Yang, Z.-D.; Lan, Y.-Q., *Nat. Commun.* **2023**, *14* (1), 593.
- (40) Lin, C.; Liu, X.; Yu, B.; Han, C.; Gong, L.; Wang, C.; Gao, Y.; Bian, Y.; Jiang, J., *ACS Appl. Mater. Interfaces* **2021**, *13* (23), 27041-27048.
- (41) Wang, M.; Wang, Z.; Shan, M.; Wang, J.; Qiu, Z.; Song, J.; Li, Z., *Chem. Mater.* **2023**, *35* (14), 5368-5377.
- (42) Li, C.; Liu, J.; Li, H.; Wu, K.; Wang, J.; Yang, Q., *Nat. Commun.* **2022**, *13* (1), 2357.
- (43) Zhou, T.; Huang, X.; Mi, Z.; Zhu, Y.; Wang, R.; Wang, C.; Guo, J., *Polym. Chem.* **2021**, *12* (22), 3250-3256.
- (44) Qian, K.; Guan, X.; Sun, N.; Jiang, H.-L., *Sci. China Chem.* **2023**, *66* (2), 436-442.
- (45) Ren, X.; Li, C.; Kang, W.; Li, H.; Ta, N.; Ye, S.; Hu, L.; Wang, X.; Li, C.; Yang, Q., *CCS Chemistry* **2021**, *4* (7), 2429-2439.
- (46) (a) Zhang, W.; Smith, J.; Hamilton, R.; Heeney, M.; Kirkpatrick, J.; Song, K.; Watkins, S. E.; Anthopoulos, T.; McCulloch, I., *J. Am. Chem. Soc.* **2009**, *131* (31), 10814-10815; (b) Sprick, R. S.; Bonillo, B.; Clowes, R.; Guiglion, P.; Brownbill, N. J.; Slater, B. J.; Blanc, F.; Zwijnenburg, M. A.; Adams, D. J.; Cooper, A. I., *Angew. Chem. Int. Ed.* **2016**, *55* (5), 1792-1796.
- (47) Hu, J.; Chen, C.; Yang, H.; Yang, F.; Qu, J.; Yang, X.; Sun, W.; Dai, L.; Li, C. M., *Appl. Catal., B Environ.* **2022**, *317*, 121723.
- (48) (a) Fu, S.; Jin, E.; Hanayama, H.; Zheng, W.; Zhang, H.; Di Virgilio, L.; Addicoat, M. A.; Mezger, M.; Narita, A.; Bonn, M.; Müllen, K.; Wang, H. I., *J. Am. Chem. Soc.* **2022**, *144* (16), 7489-7496; (b) Schweicher, G.; Garbay, G.; Jouclas, R.; Vibert, F.; Devaux, F.; Geerts, Y. H., *Adv. Mater.* **2020**, *32* (10), 1905909.
- (49) Wang, G.-B.; Zhu, F.-C.; Lin, Q.-Q.; Kan, J.-L.; Xie, K.-H.; Li, S.; Geng, Y.; Dong, Y.-B., *Chem. Commun.* **2021**, *57* (36), 4464-4467.
- (50) Chen, W.; Wang, L.; Mo, D.; He, F.; Wen, Z.; Wu, X.; Xu, H.; Chen, L., *Angew. Chem. Int. Ed.* **2020**, *59* (39), 16902-16909.
- (51) Li, Z.; Zhou, Y.; Xie, M.; Cheng, H.; Wang, T.; Chen, J.; Lu, Y.; Tian, Z.; Lai, Y.; Yu, G., *Angew. Chem.* **2023**, *135* (26), e202217815.
- (52) (a) Zhao, D.; Wang, Y.; Dong, C.-L.; Huang, Y.-C.; Chen, J.; Xue, F.; Shen, S.; Guo, L., *Nature Energy* **2021**, *6* (4), 388-397; (b) Mo, Z.; Di, J.; Yan, P.; Lv, C.; Zhu, X.; Liu, D.; Song, Y.; Liu, C.; Yu, Q.; Li, H.; Lei, Y.; Xu, H.; Yan, Q., *Small* **2020**, *16* (48), 2003914.
- (53) (a) Wang, C.; Zhang, H.; Luo, W.; Sun, T.; Xu, Y., *Angew. Chem. Int. Ed.* **2021**, *60* (48), 25381-25390; (b) Zhang, S.; Cheng, G.; Guo, L.; Wang, N.; Tan, B.; Jin, S., *Angew. Chem. Int. Ed.* **2020**, *59* (15), 6007-6014.
- (54) (a) Han, J.; Zhu, Z.; Li, N.; Chen, D.; Xu, Q.; Li, H.; He, J.; Lu, J., *Appl. Catal., B Environ.* **2021**, *291*, 120108; (b) Yan, Y.; Yu, X.; Shao, C.; Hu, Y.; Huang, W.; Li, Y., *Adv. Funct. Mater.* **2023**, 2304604.
- (55) (a) Liu, Y.; Wu, J.; Wang, F., *Appl. Catal., B Environ.* **2022**, *307*, 121144; (b) Li, Z.; Deng, T.; Ma, S.; Zhang, Z.; Wu, G.; Wang, J.; Li, Q.; Xia, H.; Yang, S.-W.; Liu, X., *J. Am. Chem. Soc.* **2023**, *145* (15), 8364-8374.

## Biosketches

	<p>Ping Xue received her Ph.D. degrees from Hubei University (2022). She is currently a lecturer at Hubei University of Science and Technology. She focuses on construction of functional porous framework materials for photocatalysis.</p>
	<p>Mingyuan Li received his Ph.D. degree from Hubei University (2022). He is currently working as a postdoctoral researcher in the group of Prof. Zhuang at Wuhan University. He is focusing on synthesized and modified metal-organic frameworks and their photoelectrocatalytic properties.</p>
	<p>Mi Tang received his Ph.D. degrees from East China University of Science and Technology (2016). During 2016-2019, he worked as a postdoctoral researcher in the group of Prof. Chengliang Wang at Huazhong University of Science and Technology (HUST). He is currently a lecturer at Hubei University. He is focusing on synthesis and characterization of organic compounds for metal-ion batteries and photocatalysis.</p>
	<p>Zhengbang Wang is currently a professor at Hubei University. He received his PhD from Karlsruhe Institute of Technology (KIT) in 2015 under supervision of Prof. Christof Wöll. Afterward, he continued working together with Prof. Wöll as a postdoctoral researcher at KIT. In 2017, he moved back to China and was appointed as Chutian Professor at Hubei University. His research interests include metal-organic framework thin films, new style porous polymer thin films, and their applications in the fields of energy and environment.</p>
	<p>Chengliang Wang is a Professor at HUST. He received his Bachelor degree from Nanjing University in 2005 and Ph.D. degree from the Institute of Chemistry, Chinese Academy of Sciences, in 2010. He then worked at the Chinese University of Hong Kong, University of Muenster, and Technical University of Ilmenau. He was selected in the National 1000-Talents Scholars and joined HUST as a Professor in 2016. He focuses on novel conjugated organic and polymeric materials for optoelectronics and batteries.</p>